

**Interpolation estimate for a finite element space with embedded discontinuities**

Journal:	<i>IMA Journal of Numerical Analysis</i>
Manuscript ID:	IMAJNA-ES-2010-077.R1
Manuscript Type:	Original Manuscript
Date Submitted by the Author:	02-Nov-2010
Complete List of Authors:	Buscaglia, Gustavo; University of Sao Paulo, ICMC Agouzal, Abdellatif; Univ. Claude Bernard - Lyon I, ICJ
Keywords:	embedded discontinuities, interpolation, surface tension

SCHOLARONE™  
Manuscripts

# Interpolation estimate for a finite element space with embedded discontinuities

Gustavo C. Buscaglia<sup>a</sup> and Abdellatif Agouzal<sup>b</sup>

<sup>a</sup>*Instituto de Ciências Matemáticas e de Computação, Universidade de São Paulo, 13560-970 Brazil, [gustavo.buscaglia@icmc.usp.br](mailto:gustavo.buscaglia@icmc.usp.br)*

<sup>b</sup>*ICJ, Université Claude Bernard, Lyon I, 69622 Villeurbanne, France, [agouzal@univ-lyon1.fr](mailto:agouzal@univ-lyon1.fr)*

---

## Abstract

We consider a recently proposed finite element space, which consists of piecewise affine functions with discontinuities across a smooth given interface  $\Gamma$  (a curve in 2D, a surface in 3D). Contrary to existing XFEM and related methodologies, the space is a variant of the standard conforming  $\mathbb{P}_1$  space which can be implemented element by element. Further, it neither introduces new unknowns nor deteriorates the sparsity structure.

It is proved that, for  $u$  arbitrary in  $W^{1,p}(\Omega \setminus \Gamma) \cap W^{2,s}(\Omega \setminus \Gamma)$ , the interpolant  $\mathcal{I}_h u$  defined by this new space satisfies

$$\|u - \mathcal{I}_h u\|_{L^q(\Omega)} \leq C \left[ h^{1+\frac{1}{q}-\frac{1}{p}} |u|_{W^{1,p}(\Omega \setminus \Gamma)} + h^2 |u|_{W^{2,s}(\Omega \setminus \Gamma)} \right]$$

where  $h$  is the mesh size,  $\Omega \subset \mathbb{R}^d$  is the domain,  $p > d$ ,  $p \geq q$ ,  $s \geq q$ , and standard notation has been adopted for the function spaces.

This result proves the good approximation properties of the finite element space as compared to any space consisting of functions continuous across  $\Gamma$ , which would yield an error in the  $L^q(\Omega)$ -norm of order  $h^{\frac{1}{q}-\frac{1}{p}}$ . These properties make this space especially attractive for approximating the pressure in problems with surface tension or other immersed interfaces that lead to discontinuities in the pressure field. Further, the result remains true for interfaces that end within the domain, as happens for example in cracked domains.

*Key words:* Finite element, interpolation, interface, discontinuous pressure, cracked domain, surface tension

---

1  
2  
3 **1 Introduction**  
4  
5  
6

7 In Eulerian, fixed grid methods for fluid mechanics, interfaces that exist within  
8 the domain are not followed by the mesh. This creates difficulties in the ap-  
9 proximation of those variables that are discontinuous at the interface, a typical  
10 example being the pressure in multiphase flow with different viscosities for the  
11 phases and/or surface tension effects, or when the interface between the phases  
12 behaves as an elastic membrane.  
13  
14

15 Let  $\Gamma$  be an interface (embedded in some domain  $\Omega$ ) at which some function  
16  $u \in L^2(\Omega)$  is discontinuous, and let  $u_h$  be its  $L^2(\Omega)$ -projection onto some  
17 function space  $V_h$  which consists of functions that are *continuous* at  $\Gamma$ . Then,  
18 no matter how smooth  $u$  is outside  $\Gamma$ , the approximation order is [1,2]  
19  
20

$$21 \quad \|u - u_h\|_{L^2(\Omega)} \simeq C h^{\frac{1}{2}} \quad (1)$$

22 where  $h$  is the mesh size and  $C$ , here and later, denotes a generic constant.  
23 If  $\Gamma$  is not aligned with the mesh all standard finite element spaces, either  
24 continuous or discontinuous across interelement boundaries, suffer from this  
25 poor approximation order. The reason for this is that, in this situation, the  
26 discontinuity will pass through the element interiors, at which standard finite  
27 element interpolants are continuous (typically polynomial).  
28  
29  
30

31 Some attempts have been made in the last years to devise spaces with improved  
32 approximation properties. Gross & Reusken [1] recently proposed to adopt an  
33 XFEM ([3]) enrichment of the pressure space, incorporating functions that  
34 are discontinuous at  $\Gamma$ , as had also been proposed by Minev *et al* [4]. They  
35 obtained improved ( $h^2$ ) convergence order at the expense of the well-known  
36 pitfalls of the XFEM methodology: The ill-conditioning of the system matrix  
37 due to approximate linear dependence of the basis, and the introduction of  
38 new unknowns that depend on the location of the interface, thus requiring  
39 the code to completely rebuild the linear system structure for each interface  
40 location.  
41  
42  
43  
44

45 In this article we analyze an alternative approach due to Ausas *et al* [5],  
46 which has some interesting properties: (a) It is a modification of the standard,  
47 continuous  $P_1$  finite element space, with exactly the same unknowns and con-  
48 nectivity; (b) the modified basis functions can be computed at the element  
49 level, making its implementation straightforward in existing codes; (c) its ap-  
50 proximation order (in the  $L^2(\Omega)$ -norm) is  $h^{\frac{3}{2}}$ , which is lower than that of the  
51 XFEM space but is one order higher than that of any standard space; and  
52 (d) its approximation order is already higher than the velocity approximation  
53 order of the mini-element ([6]) or of stabilized  $P_1/P_1$  formulations ([7,8]), both  
54 of order at most  $h$ , so that using this space for the pressure has no adverse  
55 effect on the overall velocity-pressure approximation. In this last regard, we  
56  
57  
58  
59  
60

remind the reader that the natural error measure for Stokes or Navier-Stokes problems is the sum of the  $H^1(\Omega)$ -error for velocity and the  $L^2(\Omega)$ -error for pressure. The result is established here in the more general  $L^q(\Omega)$ -setting,  $q \geq 1$ , because this entails no additional difficulties.

## 2 Description of the finite element space

We first analyze the case in which  $\Gamma$  does not end within the domain, and later discuss the modification required in the case in which  $\Gamma$  is crack-like.

Let  $V_h$  be the standard, conforming  $P_1$  finite element space defined on a triangulation  $\mathcal{T}_h$  of  $\Omega$ . The idea behind the space proposed by Ausas *et al* [5], denoted by  $W_h$  from now on, is quite simple: To begin with, in those elements that are not cut by  $\Gamma$  the space  $W_h$  coincides with  $V_h$  and the basis functions are simply those of the conforming  $P_1$  finite element space. In the elements that intersect  $\Gamma$ , each edge  $E$  (in both 2D and 3D the segments joining nodes of  $\mathcal{T}_h$  are referred to as *edges*) cut by  $\Gamma$  is divided into two parts,  $E^+$  and  $E^-$ , according to the side of  $\Gamma$  on which the part lies. The functions in  $W_h$  are then defined by their values at the original nodes of the mesh plus the new nodes created at the intersections of the mesh edges with  $\Gamma$ . The functions in  $W_h$  are bi-valued at these new nodes, but their values there are not degrees of freedom available for interpolation. Instead, the value on each side is defined as being the same as that of the (unique) node of the original triangulation that lies on the same edge and on the same side. In the rest of this section we recall the corresponding basis functions in two dimensions, stressing some properties that are essential for our proof of the interpolation estimate. More details, together with the three-dimensional version of the basis functions, can be found in [5].

We assume that no edge of the triangulation is cut twice by  $\Gamma$ . Consider the element  $K$  to be the triangle  $ABC$ , which is cut by  $\Gamma$  at points  $P$  and  $Q$ . The (possibly curved) segment  $PQ$  divides  $K$  into two *subparts*: curved triangle  $APQ$  and curved quadrilateral  $BCQP$  (see Fig. 1).

*Remark 1. Though in most of the figures hereafter the piece of interface  $\Gamma \cap K$  is shown as a straight segment for ease of interpretation, the reader should keep in mind that  $\Gamma$  has neither been assumed to be a polygon/polyhedron nor approximated by one. The usual mapping techniques to define  $\mathbb{P}_k$  or  $\mathbb{Q}_k$  interpolants on curved elements are adopted, and it is tacitly assumed that  $\Gamma \cap K$  is sufficiently well-behaved for the mappings to be well defined. This will always be the case if the mesh size is much smaller than the local radius of curvature of  $\Gamma \cap K$ . Hereafter we also omit the word “curved” when referring to a piece of  $\Gamma$ , calling “curved triangles” simply “triangles”, etc.*

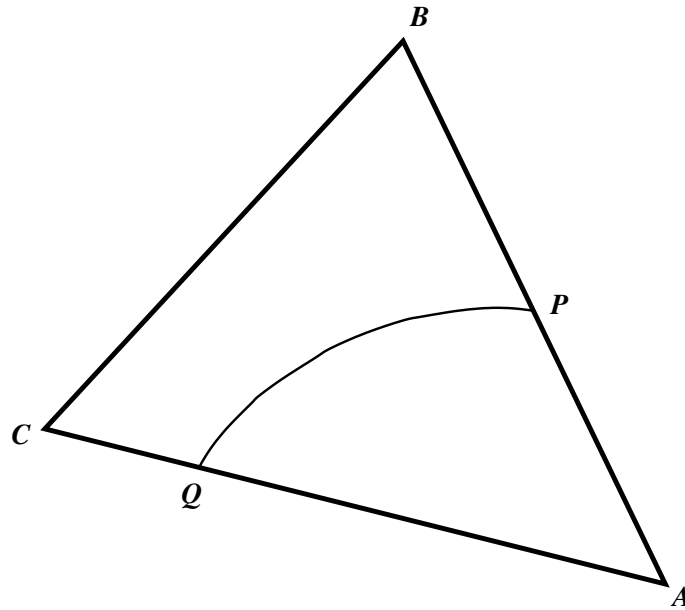


Fig. 1. Partition of a single element into subparts following the interface  $PQ$ .

Let us arbitrarily denote the triangle  $APQ$  the “plus” side of  $\Gamma$  and quadrilateral  $BCQP$  the “minus” side. One can here choose to either adopt a  $\mathbb{Q}_1$  interpolation in  $BCQP$ , or subdivide the quadrilateral into two triangles,  $BCP$  and  $CQP$ . In what follows we adopt the latter option.

Three nodal basis functions,  $\varphi_A$ ,  $\varphi_B$  and  $\varphi_C$ , can then be defined satisfying the following properties:

**P1**  $\varphi_\alpha(\beta) = 1$  if  $\alpha = \beta$  and zero otherwise, where  $\alpha$  and  $\beta$  can take the values  $A$ ,  $B$  or  $C$ .

**P2**  $\varphi_A + \varphi_B + \varphi_C = 1$ .

**P3** At any point of  $K$ , the values of  $\varphi_A$ ,  $\varphi_B$  and  $\varphi_C$  lie between zero and one.

**P4** Though not necessary for our interpolation result, it is also true that when combined with the corresponding basis functions of the neighbor elements, the resulting functions are continuous everywhere outside  $\Gamma$ .

Analogous properties are satisfied by the four basis functions proposed by [5] for three-dimensional interpolation.

The basis functions are defined to be piecewise  $\mathbb{P}_1$  inside each of the subtriangles  $APQ$ ,  $BCP$  and  $CQP$ . It only remains to define their values at the vertices of the subtriangles, i.e., at the points  $A$ ,  $B$ ,  $C$ ,  $P$  and  $Q$ , but, since they are discontinuous at  $\Gamma$ , two values (“plus” and “minus”) are given at points  $P$  and  $Q$ . These values are:

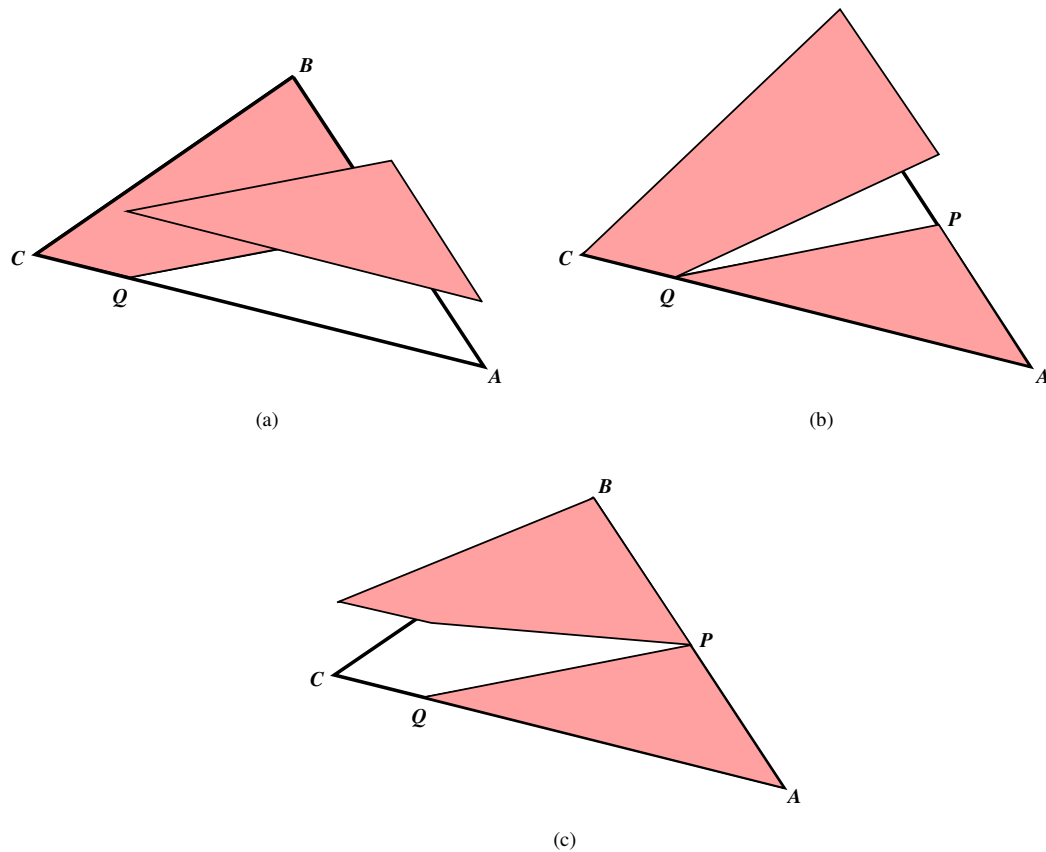


Fig. 2. Basis functions for the new finite element space: (a)  $\varphi_A$ , (b)  $\varphi_B$  and (c)  $\varphi_C$ .

$$\varphi_A(A) = 1 \quad \varphi_B(A) = 0 \quad \varphi_C(A) = 0 \quad (2)$$

$$\varphi_A(B) = 0 \quad \varphi_B(B) = 1 \quad \varphi_C(B) = 0 \quad (3)$$

$$\varphi_A(C) = 0 \quad \varphi_B(C) = 0 \quad \varphi_C(C) = 1 \quad (4)$$

$$\varphi_A(P^+) = 1 \quad \varphi_B(P^+) = 0 \quad \varphi_C(P^+) = 0 \quad (5)$$

$$\varphi_A(P^-) = 0 \quad \varphi_B(P^-) = 1 \quad \varphi_C(P^-) = 0 \quad (6)$$

$$\varphi_A(Q^+) = 1 \quad \varphi_B(Q^+) = 0 \quad \varphi_C(Q^+) = 0 \quad (7)$$

$$\varphi_A(Q^-) = 0 \quad \varphi_B(Q^-) = 0 \quad \varphi_C(Q^-) = 1 \quad (8)$$

From the first three lines above we verify that property P1 is satisfied. Since the sum of the three functions is one at all vertices, their sum is the constant function equal to one and property P2 is satisfied. The interpolation being piecewise  $\mathbb{P}_1$ , the extrema take place at the vertices and property P3 follows from direct inspection.

### 3 Interpolation estimate

Let  $\Omega \subset \mathbb{R}^d$  be an open bounded polygonal domain, and let  $\Gamma$  be a smooth curve in  $\Omega$  (a smooth surface if  $d = 3$ ) that does not end within the domain.

Let us denote by “regular” triangulation  $\mathcal{T}_h$  of  $\Omega$  a partition into simplices which has no hanging nodes (conforming triangulation) and that, in addition, satisfies the following hypotheses:

**H1** Each edge (segment that adjoins two vertices) of each simplex is cut at most once by  $\Gamma$ .

**H2** The interface  $\Gamma$  does not pass by any vertex. This is a technical assumption needed for the interpolant to be defined. The interpolation estimate does not deteriorate when the distance from  $\Gamma$  to one of the vertices tends to zero.

**H3** The mesh size  $h$  satisfies, for all  $K \in \mathcal{T}_h$ ,  $ch \leq \rho(K) \leq \text{diam}(K) \leq h$ , where  $\rho$  is the radius of the inscribed circle/sphere, and thus  $c^d h^d \leq \text{meas}(K) \leq h^d$ , with  $0 < c < 1$  independent of  $h$ . Notice that, in particular, the triangulation needs to be quasi-uniform.

**H4** The triangulation is such that, for each  $K$  and for each node  $I$  of  $K$ , the subpart that contains  $I$  (as defined in Fig. 1) is star-shaped with respect to  $I$ . This is equivalent to requiring “visibility” of  $\Gamma \cap K$  from  $I$ ; i.e., that for each  $x \in \Gamma \cap K$  the straight segment  $\overline{xI}$  only intersects  $\Gamma$  at  $x$ .

*Notation:* From now on, for any measurable set  $\omega$ , we will denote

$$|\omega| = \text{meas}(\omega).$$

For  $u \in W^{1,p}(\Omega \setminus \Gamma)$  (with  $p > d$ , so that functions are continuous in  $\Omega \setminus \Gamma$ ), let  $\mathcal{I}_h u$  be the interpolant of  $u$  in  $W_h$ , defined by

$$\mathcal{I}_h u(x) = \sum_{i=1}^{N_V} u(X_i) \varphi_i(x) \tag{9}$$

where  $x \in \Omega$ ,  $N_V$  is the number of vertices and  $\varphi_i$  is the basis function associated to vertex (node) number  $i$ , which is located at  $X_i \in \mathbb{R}^d$ .

This section is devoted to the proof of the following estimate:

**Theorem 3.1.** *Let  $p, q$  and  $s$  be three given real numbers satisfying  $p > d$ ,  $1 \leq q \leq p$  and  $s \geq q$ . Then there exists a constant  $C$  such that, for all regular triangulations  $\mathcal{T}_h$  of  $\Omega$ , and for all  $u \in W^{1,p}(\Omega \setminus \Gamma) \cap W^{2,s}(\Omega \setminus \Gamma)$ ,*

$$\|u - \mathcal{I}_h u\|_{L^q(\Omega)} \leq C \left[ h^{1+\frac{1}{q}-\frac{1}{p}} |u|_{W^{1,p}(\Omega \setminus \Gamma)} + h^2 |u|_{W^{2,s}(\Omega \setminus \Gamma)} \right] \tag{10}$$

For the proof we first establish some lemmata.

**Lemma 3.2.** *Let  $\omega$  be a bounded open set in  $\mathbb{R}^d$ . Let  $p > d$  and let  $y \in \overline{\omega}$  be a point such that  $\omega$  is star-shaped with respect to  $y$ . Then, for all  $w \in L^p(\omega)$ ,*

$$\int_{\omega} \left[ \int_0^1 |w(y + t(x - y))| dt \right]^p dx \leq \left( \frac{p}{p-d} \right)^p \|w\|_{L^p(\omega)}^p \tag{11}$$

*Proof.* Notice first that the integral on the left makes sense, since  $y+t(x-y) \in \omega$  for all  $t \in (0, 1)$  because  $\omega$  is star-shaped with respect to  $y$ . Without loss of generality we take  $y = 0$ . Let  $q$  be such that  $\frac{1}{p} + \frac{1}{q} = 1$ . We multiply and divide by  $t^\alpha$ , where  $\alpha = \frac{(p-1)d}{p^2}$ , to obtain

$$\begin{aligned} \int_{\omega} \left[ \int_0^1 |w(tx)| dt \right]^p dx &= \int_{\omega} \left[ \int_0^1 |w(tx)| t^\alpha t^{-\alpha} dt \right]^p dx \\ &\leq \int_{\omega} \left( \int_0^1 |w(tx)|^p t^{\alpha p} dt \right) \left( \int_0^1 t^{-\alpha q} dt \right)^{\frac{p}{q}} dx \\ &= \left( \frac{1}{1 - \alpha q} \right)^{\frac{p}{q}} \int_{\omega} \int_0^1 |w(tx)|^p t^{\alpha p} dt dx \\ &= \left( \frac{p}{p-d} \right)^{p-1} \int_{\omega} \int_0^1 |w(z)|^p t^{\alpha p-d} dt dz \\ &= \left( \frac{p}{p-d} \right)^p \|w\|_{L^p(\omega)}^p \end{aligned}$$

where we have used Hölder's inequality in one dimension and the change of variables  $z = tx$ , implying  $dt dz = t^d dt dx$ .  $\square$

**Lemma 3.3.** *Under the same hypotheses of Lemma 3.2 we have, for all  $1 \leq q \leq p$ ,*

$$\|w - w(y)\|_{L^q(\omega)} \leq \left( \frac{p}{p-d} \right) \text{diam}(\omega) |\omega|^{\frac{1}{q} - \frac{1}{p}} \|w\|_{W^{1,p}(\omega)} \quad (12)$$

whenever  $w \in W^{1,p}(\omega)$ .

*Proof.* The proof follows a density argument. For  $w \in C^1(\omega) \cap W^{1,p}(\omega)$  we have, for all  $x \in \omega$ ,

$$w(x) - w(y) = \int_0^1 \nabla w(y + t(x-y)) \cdot (x-y) dt$$

implying

$$\|w - w(y)\|_{L^q(\omega)}^q \leq \int_{\omega} \left| \int_0^1 \nabla w(y + t(x-y)) \cdot (x-y) dt \right|^q dx$$

From Lemma 3.2 and Hölder's inequality with  $r = \frac{p}{q}$  and  $s = \frac{p}{p-q}$  (if  $p = q$  this is of course unnecessary) we then get

$$\int_{\omega} \left| \int_0^1 \nabla w(y + t(x-y)) \cdot (x-y) dt \right|^q dx \leq \left( \frac{p}{p-d} \right)^q \text{diam}(\omega)^q |\omega|^{1 - \frac{q}{p}} \|\nabla w\|_{L^p(\omega)}^q$$

$\square$

**Lemma 3.4.** *Let  $K$  be a simplex of  $\mathcal{T}_h$  of vertices  $\{X_i\}_{i=1,\dots,d+1}$ , which is crossed by the interface  $\Gamma$ . Let  $w \in W^{1,p}(K \setminus \Gamma)$  (with  $p > d$ ), and let  $\mathcal{I}_K w(x) = \sum_{i=1}^{d+1} w(X_i) \varphi_i(x)$  be its local interpolant. Then, for all  $1 \leq q \leq p$ ,*

$$\|w - \mathcal{I}_K w\|_{L^q(K)} \leq \frac{p(d+1)}{p-d} h^{1+\frac{d}{q}-\frac{d}{p}} |w|_{W^{1,p}(K \setminus \Gamma)} \quad (13)$$

*Proof.* We start from the straightforward estimate

$$\|w - \mathcal{I}_K w\|_{L^q(K)} = \left\| \sum_{i=1}^{d+1} [w - w(X_i)] \varphi_i \right\|_{L^q(K)} \leq \sum_{i=1}^{d+1} \|w - w(X_i)\|_{L^q(K_i)}$$

where  $K_i$  denotes the support of  $\varphi_i$ . Now notice that, by construction of the basis functions,  $K_i$  is the connected component of  $\bar{K}$  (connected in the sense that lies on one side of  $\Gamma$ ) that contains the vertex  $X_i$ , and  $K_i$  is star-shaped with respect to  $X_i$  by hypothesis H4. We thus apply Lemma 3.3 and H3 to obtain

$$\|w - \mathcal{I}_K w\|_{L^q(K)} \leq \left( \frac{p}{p-d} \right) h^{1+\frac{d}{q}-\frac{d}{p}} \sum_{i=1}^{d+1} |w|_{W^{1,p}(K_i)}$$

from which the result follows.  $\square$

We also recall the following classical estimate for  $\mathbb{P}_1$  elements, which holds for all elements not intersected by  $\Gamma$ .

**Lemma 3.5.** *There exists  $c_s > 0$  such that, for all  $K \in \mathcal{T}_h$  and all  $w \in W^{2,s}(K)$ , we have*

$$\|w - \mathcal{I}_K w\|_{L^q(K)} \leq c_s h^{2+\frac{d}{q}-\frac{d}{s}} |w|_{W^{2,s}(K)} \quad (14)$$

We now proceed to the proof of Theorem 3.1.

*Proof.* We begin by decomposing the mesh  $\mathcal{T}_h$  into the subset of elements  $\mathcal{R}_h$  of elements *not intersected* by  $\Gamma$ , and the subset  $\mathcal{S}_h$  of elements *intersected* by  $\Gamma$ . Because of the quasi-uniformity of the mesh, we know that the number of elements in  $\mathcal{R}_h$  is  $N_{\mathcal{R}_h} \leq ch^{-d}$ , while the regularity of  $\Gamma$  makes that  $N_{\mathcal{S}_h} \leq ch^{-d+1}$ , where  $c$  does not depend on  $h$ . We will estimate the two terms in

$$\begin{aligned} \|u - \mathcal{I}_h u\|_{L^q(\Omega)} &= \left( \sum_{K \in \mathcal{T}_h} \|u - \mathcal{I}_K u\|_{L^q(K)}^q \right)^{\frac{1}{q}} \\ &\leq \left( \sum_{K \in \mathcal{R}_h} \|u - \mathcal{I}_K u\|_{L^q(K)}^q \right)^{\frac{1}{q}} + \left( \sum_{K \in \mathcal{S}_h} \|u - \mathcal{I}_K u\|_{L^q(K)}^q \right)^{\frac{1}{q}} \end{aligned} \quad (15)$$

The first term consists of classical  $\mathbb{P}_1$  elements, so that from Lemma 3.5 we have

$$\begin{aligned} \sum_{K \in \mathcal{R}_h} \|u - \mathcal{I}_K u\|_{L^q(K)}^q &\leq c_s^q h^{2q+d-\frac{dq}{s}} \sum_{K \in \mathcal{R}_h} |u|_{W^{2,s}(K)}^q \\ &\leq c_s^q h^{2q+d-\frac{dq}{s}} N_{\mathcal{R}_h}^{1-\frac{q}{s}} \left( \sum_{K \in \mathcal{R}_h} |u|_{W^{2,s}(K)}^s \right)^{\frac{q}{s}} \\ &\leq c_s^q h^{2q} |u|_{W^{2,s}(\Omega \setminus \Gamma)}^q \end{aligned} \quad (16)$$

Turning now to the second term in (15), we have from Lemma 3.4,

$$\begin{aligned} \sum_{K \in \mathcal{S}_h} \|u - \mathcal{I}_K u\|_{L^q(K)}^q &\leq \left( \frac{p(d+1)}{p-d} \right)^q h^{q+d-\frac{dq}{p}} \sum_{K \in \mathcal{S}_h} |u|_{W^{1,p}(K \setminus \Gamma)}^q \\ &\leq \left( \frac{p(d+1)}{p-d} \right)^q h^{q+d-\frac{dq}{p}} N_{\mathcal{S}_h}^{1-\frac{q}{p}} \left( \sum_{K \in \mathcal{S}_h} |u|_{W^{1,p}(K \setminus \Gamma)}^p \right)^{\frac{q}{p}} \\ &\leq c^{1-\frac{q}{p}} \left( \frac{p(d+1)}{p-d} \right)^q h^{q+1-\frac{q}{p}} |u|_{W^{1,p}(\Omega \setminus \Gamma)}^q \end{aligned} \quad (17)$$

Combining now (15)-(17) we obtain the claimed result.  $\square$

*Remark 2.* Notice that the proof does not depend on  $d$  being equal to two. The estimate is thus also proved for the three-dimensional case.

#### 4 Cracked domains

In the case of an interface  $\Gamma$  that ends within the domain we have yet to define the interpolant for those elements that contain endpoints of the interface. Consider the triangle  $ABC$  as shown in Fig. 3. The interface ends at point  $T$ , but point  $Q$  can still be defined by suitably continuing the segment  $PT$ , and the subdivision of the element is identical to the previous case. The simplest possibility is to adopt the same basis functions as in the fully-cut case, in which case Theorem 3.1 applies without any modification in the proof.

However, if the basis functions of the fully-cut element are used, property P4 does not hold. The interpolant  $\mathcal{I}_h u$  is discontinuous not only at  $\Gamma$  but also along the edge  $AC$ , since  $\varphi_A$  and  $\varphi_C$  are different as seen from the two elements that share edge  $AC$ . For some formulations, such as those that make use of the pressure Poisson equation, it is classical to have  $W_h \in H^1(\Omega \setminus \Gamma)$ . This will not hold with the interpolant proposed above because of the discontinuities at the

partially-cut elements just discussed. A special treatment for the partially-cut elements is thus needed.

As explained by Ausas *et al* [5], continuity everywhere outside  $\Gamma$  can easily be recovered in both two and three dimensions without deteriorating the accuracy of the interpolation. The basis functions needed for this fix, which are piecewise  $\mathbb{P}_1$  inside each of the subtriangles  $APQ$ ,  $BCP$  and  $CQP$  as before, are defined to be continuous along the edge  $AC$  as follows: Let

$$a = \frac{|CQ|}{|AC|},$$

then,

$$\varphi_A(A) = 1 \quad \varphi_B(A) = 0 \quad \varphi_C(A) = 0 \tag{18}$$

$$\varphi_A(B) = 0 \quad \varphi_B(B) = 1 \quad \varphi_C(B) = 0 \tag{19}$$

$$\varphi_A(C) = 0 \quad \varphi_B(C) = 0 \quad \varphi_C(C) = 1 \tag{20}$$

$$\varphi_A(P^+) = 1 \quad \varphi_B(P^+) = 0 \quad \varphi_C(P^+) = 0 \tag{21}$$

$$\varphi_A(P^-) = 0 \quad \varphi_B(P^-) = 1 \quad \varphi_C(P^-) = 0 \tag{22}$$

$$\varphi_A(Q) = a \quad \varphi_B(Q) = 0 \quad \varphi_C(Q) = 1 - a \tag{23}$$

The corresponding functions are plotted in Fig. 4. Notice that  $\varphi_C$  is nothing but the standard  $\mathbb{P}_1$  basis function, since the interface does not intersect any edge containing point  $C$ .

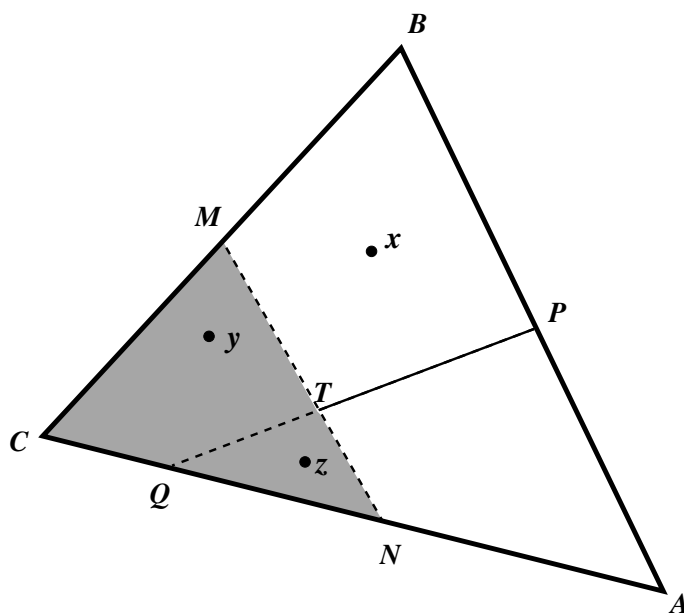


Fig. 3. Scheme of an element (the triangle  $ABC$ ) containing an endpoint  $T$  of the interface, which is represented by the segment  $PT$ .

It is easily checked that this basis satisfies properties P1-P4 above. A three-dimensional version, also satisfying the same properties, has also been intro-

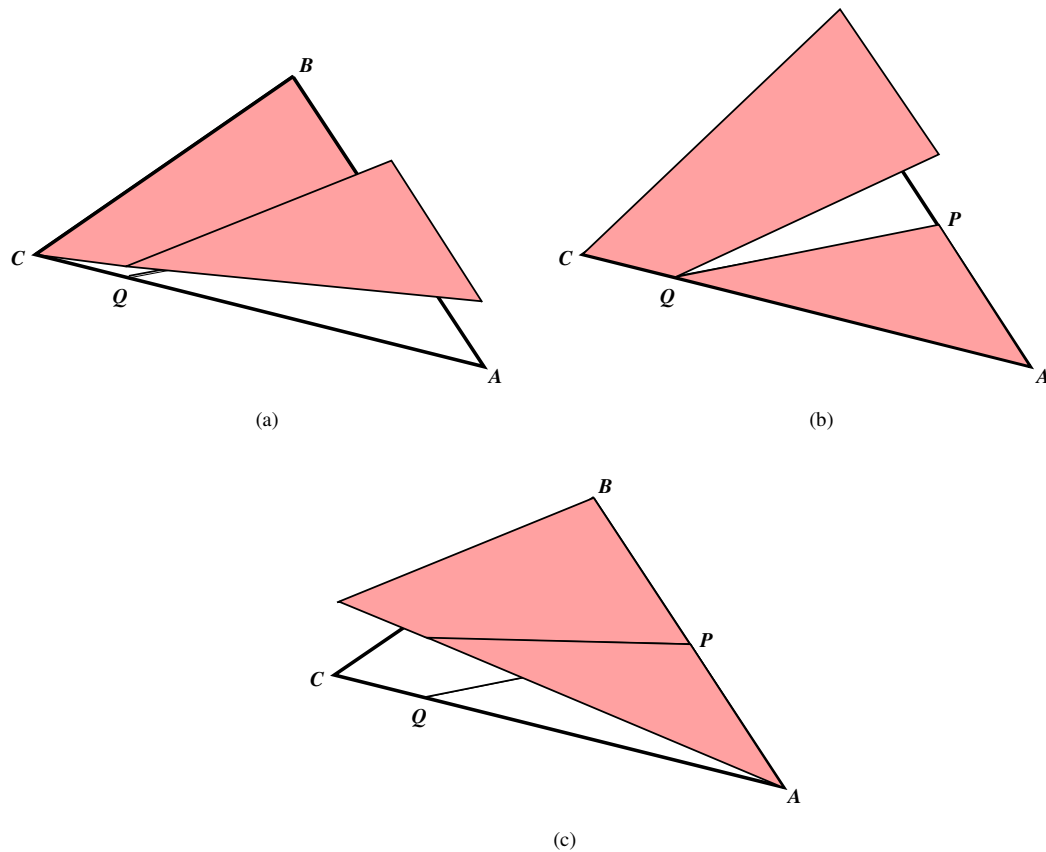


Fig. 4. Basis functions for a “cracked” element: (a)  $\varphi_A$ , (b)  $\varphi_B$  and (c)  $\varphi_C$ .

duced[5]. The rest of this section is devoted to extending the interpolation estimate to this case. There exist now three subsets of elements:  $\mathcal{R}_h$ , those *not intersected* by  $\Gamma$ ,  $\mathcal{S}_h$ , those *fully cut* by  $\Gamma$ , and  $\mathcal{Z}_h$ , those *partially cut* by  $\Gamma$  in which the new basis has been adopted.

This last subset is the only novelty with respect to the proof of Lemma 3.5. In particular, from the quasi-uniformity of the mesh and the regularity of  $\Gamma$  we assume that the number of elements in  $\mathcal{Z}_h$  is  $N_{\mathcal{Z}_h} \leq c_z h^{-d+2}$ . In particular, in two dimensions the number of endpoints of  $\Gamma$  is assumed finite.

Our purpose is to prove that *Theorem 3.1 still holds if  $\Gamma$  ends within the domain and the basis defined by (18)-(23) is adopted in the partially-cut elements.*

We begin, as in the previous proof, by decomposing

$$\begin{aligned} \|u - \mathcal{I}_h u\|_{L^q(\Omega)} &\leq \left( \sum_{K \in \mathcal{R}_h} \|u - \mathcal{I}_K u\|_{L^q(K)}^q \right)^{\frac{1}{q}} + \\ &+ \left( \sum_{K \in \mathcal{S}_h} \|u - \mathcal{I}_K u\|_{L^q(K)}^q \right)^{\frac{1}{q}} + \\ &+ \left( \sum_{K \in \mathcal{Z}_h} \|u - \mathcal{I}_K u\|_{L^q(K)}^q \right)^{\frac{1}{q}} \end{aligned} \quad (24)$$

Since the bounds for the two first terms have already been established, it only remains to show that there exists a constant  $C$  such that

$$\left( \sum_{K \in \mathcal{Z}_h} \|u - \mathcal{I}_K u\|_{L^q(K)}^q \right)^{\frac{1}{q}} \leq C h^{1+\frac{1}{q}-\frac{1}{p}} |u|_{W^{1,p}(\Omega \setminus \Gamma)} \quad (25)$$

The difficulty lies in that Lemma 3.4 does not hold for this new interpolant, because it is based on applying Lemma 3.3 to the open set

$$\{x \in K \setminus \Gamma \mid \varphi_A(x) \neq 0\}$$

which with the new basis is not star-shaped with respect to  $A$ . As depicted in Fig. 3, points  $x$  exist with  $\varphi_A(x) \neq 0$  and such that the straight segment  $\overline{x\bar{A}}$  intersects  $\Gamma$ , making the argument of Lemma 3.4 invalid. We explain here how to tackle this difficulty in the case of a straight interface ( $PT$  is a straight segment). Its extension to the curved case is not difficult but requires some technicalities.

The idea is to construct a path that avoids crossing  $\Gamma$ . For that purpose, let us denote by  $\Delta_1$  the triangle  $APQ$ , by  $\Delta_2$  the quadrilateral  $BCQP$ , and let us define a third convex set,  $\Delta_3$  (in Fig. 3 it corresponds to the triangle  $CNM$ ) which overlaps with the other two. Further, we define  $\omega_1 = \Delta_1 \cap \Delta_3$  and  $\omega_2 = \Delta_2 \cap \Delta_3$ . Our path from the point  $x$  to  $A$  will consist of three segments:  $\overline{xy}$ , with  $y \in \omega_2$ , then  $\overline{yz}$ , with  $z \in \omega_1$ , and finally  $\overline{z\bar{A}}$ . With these definitions, Lemma 3.5 is adapted to the partially-cut element as follows:

**Lemma 4.1.** *Let  $K$  be a partially-cut element and let  $A$  be a vertex. Then, for  $p > d$  and  $1 \leq q \leq p$ ,*

$$\|w - w(A)\|_{L^q(K)} \leq \frac{2p}{p-d} \left[ 1 + \left( \frac{|\Delta_2|}{|\omega_1|} \right)^{\frac{1}{q}} \right] \text{diam}(K) |K|^{\frac{1}{q}-\frac{1}{p}} |w|_{W^{1,p}(K \setminus \Gamma)} \quad (26)$$

*Proof.* We begin by decomposing

$$\|w - w(A)\|_{L^q(K)} \leq \|w - w(A)\|_{L^q(\Delta_1)} + \|w - w(A)\|_{L^q(\Delta_2)} \quad (27)$$

Since  $\Delta_1$  is convex and  $A \in \overline{\Delta_1}$ , Lemma 3.3 immediately provides a suitable bound for the first term; i.e.,

$$\|w - w(A)\|_{L^q(\Delta_1)} \leq \frac{p}{p-d} \text{diam}(\Delta_1) |\Delta_1|^{\frac{1}{q}-\frac{1}{p}} |w|_{W^{1,p}(\Delta_1)} \quad (28)$$

We thus now turn to the second term,

$$\begin{aligned} \|w - w(A)\|_{L^q(\Delta_2)}^q &= \int_{\Delta_2} |w(x) - w(A)|^q dx = \\ &= \frac{1}{|\omega_1| |\omega_2|} \int_{\omega_1} \int_{\omega_2} \int_{\Delta_2} |w(x) - w(y) + w(y) - w(z) + w(z) - w(A)|^q dx dy dz \end{aligned}$$

defining  $\mathcal{B} = \Delta_2 \times \omega_2 \times \omega_1$  and with  $F_1(x, y, z) = w(x) - w(y)$ ,  $F_2(x, y, z) = w(y) - w(z)$  and  $F_3(x, y, z) = w(z) - w(A)$  we arrive at

$$\begin{aligned} \|w - w(A)\|_{L^q(\Delta_2)} &= \frac{1}{(|\omega_1| |\omega_2|)^{\frac{1}{q}}} \|F_1 + F_2 + F_3\|_{L^q(\mathcal{B})} \\ &\leq \frac{1}{(|\omega_1| |\omega_2|)^{\frac{1}{q}}} \left( \|F_1\|_{L^q(\mathcal{B})} + \|F_2\|_{L^q(\mathcal{B})} + \|F_3\|_{L^q(\mathcal{B})} \right) \quad (29) \end{aligned}$$

Now we establish bounds for each term. In particular, since both  $x$  and  $y$  belong to  $\Delta_2$ , we have from Lemma 3.3,

$$\begin{aligned} \|F_1\|_{L^q(\mathcal{B})}^q &= \int_{\omega_1} \int_{\omega_2} \int_{\Delta_2} |w(x) - w(y)|^q dx dy dz \\ &\leq |\omega_1| |\omega_2| c_p^q \text{diam}(\Delta_2)^q |\Delta_2|^{1-\frac{q}{p}} |w|_{W^{1,p}(\Delta_2)}^q \quad (30) \end{aligned}$$

where we have denoted  $c_p = p/(p-d)$ . Similarly,

$$\begin{aligned} \|F_2\|_{L^q(\mathcal{B})}^q &= \int_{\omega_1} \int_{\omega_2} \int_{\Delta_2} |w(y) - w(z)|^q dx dy dz \\ &\leq |\Delta_2| |\omega_2| c_p^q \text{diam}(\Delta_3)^q |\Delta_3|^{1-\frac{q}{p}} |w|_{W^{1,p}(\Delta_3)}^q \quad (31) \end{aligned}$$

and

$$\begin{aligned} \|F_3\|_{L^q(\mathcal{B})}^q &= \int_{\omega_1} \int_{\omega_2} \int_{\Delta_2} |w(z) - w(A)|^q dx dy dz \\ &\leq |\Delta_2| |\omega_2| c_p^q \text{diam}(\Delta_1)^q |\Delta_1|^{1-\frac{q}{p}} |w|_{W^{1,p}(\Delta_1)}^q \quad (32) \end{aligned}$$

Inserting now (29)-(32) and (28) into (27) the claim is proved.  $\square$

To complete the proof of (25) we proceed as in Lemmata 3.4 and 3.5, adding up the contributions of all elements in  $\mathcal{Z}_h$ , to get

$$\left( \sum_{K \in \mathcal{Z}_h} \|u - \mathcal{I}_K u\|_{L^q(K)}^q \right)^{\frac{1}{q}} \leq \mathcal{A}(h) h^{1+\frac{1}{q}-\frac{1}{p}} |u|_{W^{1,p}(\Omega \setminus \Gamma)} \quad (33)$$

where

$$\mathcal{A}(h) = \frac{2c_z p(d+1)}{p-d} \max_{K \in \mathcal{Z}_h} \left( 1 + \frac{|\Delta_2(K)|^{\frac{1}{q}}}{|\omega_1(K)|^{\frac{1}{q}}} \right) h^{\frac{1}{q}-\frac{1}{p}} \quad (34)$$

which implies (25) under the *technical* assumption that the family of triangulations  $\mathcal{T}_h$  is such that there exists a constant  $C$  such that

$$\mathcal{A}(h) \leq C \quad \forall h > 0.$$

This technical assumption in practice requires that the interface does not end exactly at an edge (face in 3D), and we have never observed any pathological behavior in the interpolation when the end point lies very close to an edge. Notice that  $h^{\frac{1}{q}-\frac{1}{p}}$  tends to zero with  $h$ , so that the ratio  $|\Delta_2(K)|/|\omega_1(K)|$  may even diverge without harming the convergence order, if the divergence is mild enough.

## 5 Numerical experiments

As a complement to the numerical experiments shown in [5], let us consider the interpolation of the function

$$u(r, \theta) = r^2 e^{-4r} \sin\left(\frac{\theta}{4}\right) \quad (35)$$

where  $r$  is the distance from a point  $z$  chosen randomly in  $(-0.25, 0.25) \times (-0.25, 0.25)$  and  $\theta$  is the angle measured from some randomly chosen  $\theta_0 \in [0, 2\pi)$ . The domain  $\Omega$  is taken as  $(-2, 2) \times (-2, 2)$ . An example of the interpolated function for an unstructured mesh with  $h = 0.1$ ,  $z = (0.1, 0.2)$  and  $\theta_0 = \frac{\pi}{3}$  is shown in Fig. 5. Notice how the function becomes rough near the discontinuity line  $\Gamma$  because the interpolant is constant along the edges on each side of  $\Gamma$ .

We investigate here two issues. The first is the robustness of the interpolation with respect to the exact position of  $\Gamma$  in the mesh. For this purpose, we randomly generate 10,000 functions by varying  $z$  and  $\theta_0$ . The distribution of the interpolation error

$$e_0 = \|u - \mathcal{I}_h u\|_{L^2(\Omega)} \quad (36)$$

is shown in Fig. 6 for the mesh shown in Fig. 5 ( $h = 0.1$ ) and a refined one obtained by dividing each triangle into four ( $h = 0.05$ ). The mean  $L^2(\Omega)$ -errors for each mesh are  $4.74 \times 10^{-4}$  and  $1.46 \times 10^{-4}$ . This corresponds to a behavior of the mean of the error as  $\sim h^{1.7}$ , consistent with the one predicted by the theoretical estimate of the previous sections ( $\sim h^{1.5}$ ).

The ratio of the maximum to minimum errors are observed to be rather small, of 3.44 for the first mesh and of 2.80 for the second. The interpolation accuracy depends of course on the way the triangles are cut, but no configuration leads to a “disastrous” interpolant.

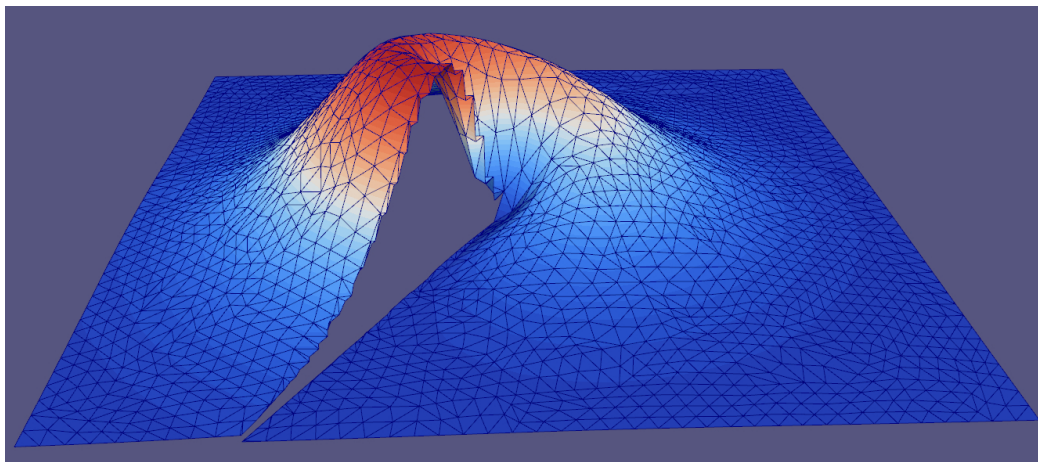
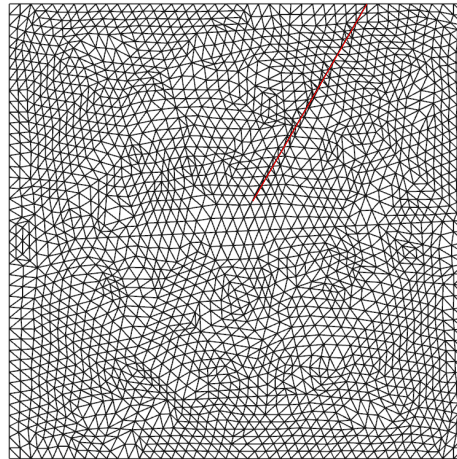


Fig. 5. Unstructured mesh with  $h = 0.1$  and discontinuous function  $u$  interpolated on it with the proposed interpolant.

The second issue investigated here is the approximation properties in  $H^1(\Omega)$ . For this purpose, we choose the same function chose above, with  $z = (0.1, 0.2)$  and  $\theta_0 = \frac{\pi}{3}$ , and perform a mesh refinement study measuring

$$e_1 = \|\nabla u - \nabla(\mathcal{I}_h u)\|_{L^2(\tilde{\Omega})} \quad (37)$$

where  $\tilde{\Omega}$  is the subset of  $\Omega$  where  $\mathcal{I}_h u$  is continuous. The results are shown

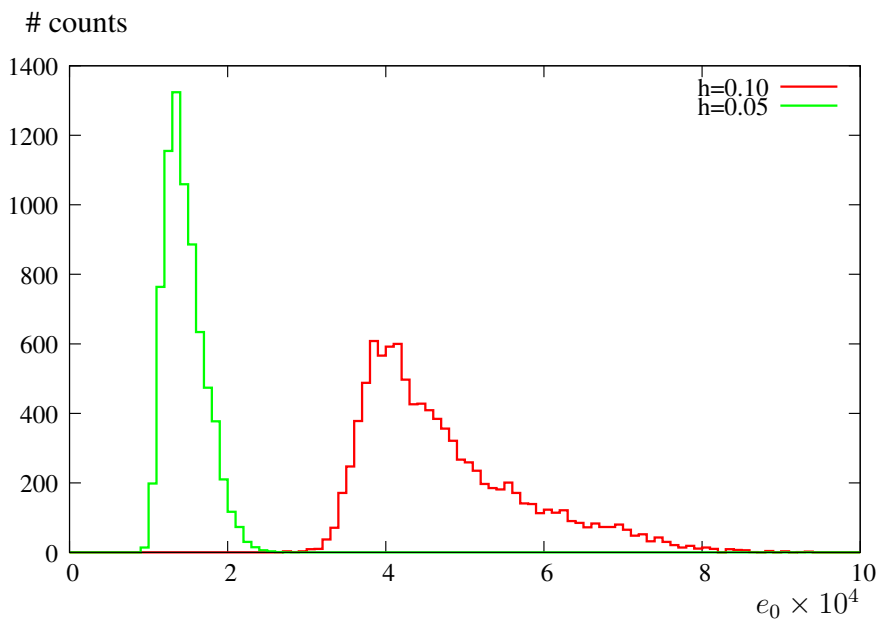


Fig. 6. Histograms of the distributions of the interpolation  $L^2(\Omega)$ -errors, for two meshes, after 10,000 random realizations.

in Fig. 7, and show evidence of an interpolation order of  $h^{\frac{1}{2}}$ , which is quite logical since in the interior of the cut elements  $\nabla u$  is not approximated at all.

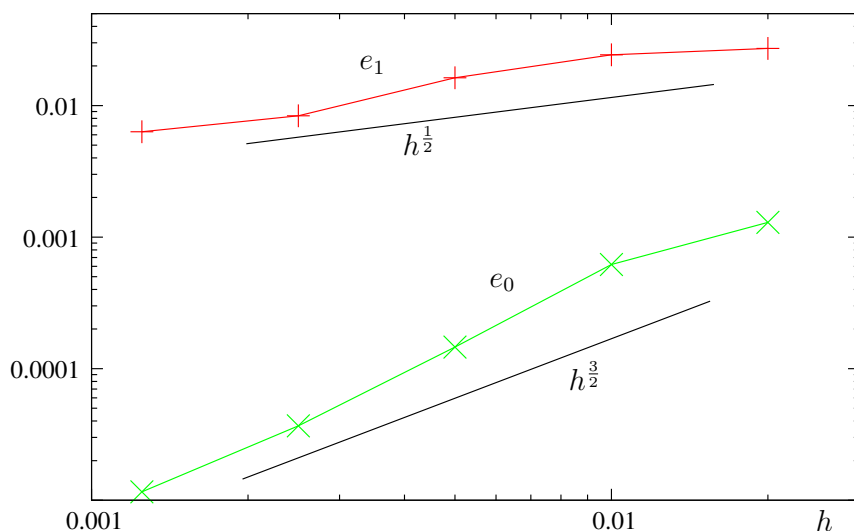


Fig. 7. Plots of the interpolation errors  $e_0$  and  $e_1$  as functions of  $h$ .

## 6 Concluding remarks

A new finite element space  $W_h$  has been analyzed, which has the same unknowns as the  $\mathbb{P}_1$ -conforming space but consists of functions that are discontinuous across a given interface  $\Gamma$ , assumed not aligned with the mesh.

1  
2  
3 The interpolation estimate yields a convergence rate in  $L^2(\Omega)$  of order  $h^{\frac{3}{2}}$   
4 for functions that are smooth outside  $\Gamma$ . This rate, which is sharp as shown  
5 by numerical experiments in [5] and the previous section, is a significant im-  
6 provement with respect to the accuracy of continuous spaces,  $\mathcal{O}(h^{\frac{1}{2}})$ , but is  
7 still suboptimal. However, such a convergence rate implies that the space  $W_h$ ,  
8 when taken as pressure space, will *not* limit the accuracy of a (Navier-)Stokes  
9 calculation neither in equal-order velocity-pressure approximations, nor in the  
10 minielement approximation. In fact, in both cases the global accuracy is lim-  
11 ited by the  $H^1(\Omega)$ -accuracy of the velocity space, which is at most  $\mathcal{O}(h)$ .  
12  
13  
14

15  
16 In the provided estimates, the interface  $\Gamma$  is assumed to be exact. In finite  
17 element applications of the space, however, the exact interface is some  $\hat{\Gamma}$ , and  
18  $\Gamma$  is a suitable approximation thereof that renders the integrals computable.  
19 Let us assume that both  $\hat{\Gamma}$  and  $\Gamma$  are sufficiently smooth and that the distance  
20 between them satisfies  
21

$$\delta := \text{dist}(\hat{\Gamma}, \Gamma) \leq C h^r \quad (38)$$

22  
23 For example, if  $\Gamma$  is piecewise affine we expect  $r = 2$ . Given a function  $\hat{u}$  which  
24 is discontinuous at  $\hat{\Gamma}$  and belongs to  $W^{1,p}(\Omega \setminus \hat{\Gamma})$ , it must be approximated  
25 by some function  $u \in W^{1,p}(\Omega \setminus \Gamma)$  before applying the interpolation estimate  
26 proved in the previous sections. This introduces an additional error which  
27 under suitable assumptions is of the order  
28  
29

$$\|\hat{u} - u\|_{L^q(\Omega)} \leq C \|\hat{u}\|_{W^{1,q}(\Omega \setminus \hat{\Gamma})} \delta^{\frac{1}{q}} \leq C h^{\frac{r}{q}}.$$

30  
31  
32 Notice that for piecewise-affine  $\Gamma$  this error, in the  $L^2$ -norm, is  $\mathcal{O}(h)$ . For the  
33 interpolation estimate  $\mathcal{O}(h^{\frac{3}{2}})$ , obtained for the exact interface case, to remain  
34 true in the case of approximate interface, it must be guaranteed that  $r \geq 3$  in  
35 (38), which can be achieved for example with a piecewise parabolic  $\Gamma$ .  
36  
37  
38  
39

#### 40 *Acknowledgments*

41  
42  
43 The authors acknowledge partial support from FAPESP (Brazil) and CNPq  
44 (Brazil). This work was completed during a kind invitation of GCB at the  
45 INSA de Lyon, which is gratefully acknowledged. Many helps are due to  
46 Roberto Ausas, who carried out the numerical tests.  
47  
48  
49

#### 50 **References**

- 51  
52  
53  
54  
55 [1] S. Gross and A. Reusken. An extended pressure finite element space for two-  
56 phase incompressible flows with surface tension. *J. Comput. Phys.*, 224:40–58,  
57 2007.  
58  
59  
60

1  
2  
3 [2] S. Ganesan, G. Matthies, and L. Tobiska. On spurious velocities in incompressible  
4 flow problems with interfaces. *Comput. Methods Appl. Mech. Engrg.*, 196:1193–  
5 1202, 2007.  
6  
7 [3] T. Belytschko, N. Moës, S. Usui, and C. Parimi. Arbitrary discontinuities in  
8 finite elements. *Int. J. Numer. Meth. Engrng*, 50:993–1013, 2001.  
9  
10 [4] P. D. Mineev, T. Chen, and K. Nandakumar. A finite element technique for  
11 multifluid incompressible flow using Eulerian grids. *J. Comput. Phys.*, 187:255–  
12 273, 2003.  
13  
14 [5] R. Ausas, F. Simeoni de Sousa, and G. Buscaglia. An improved finite element  
15 space for discontinuous pressures. *Comput. Methods Appl. Mech. Engrg.*,  
16 199:1019–1031, 2010.  
17  
18 [6] D. Arnold, F. Brezzi, and M. Fortin. A stable finite element for the Stokes  
19 equations. *Calcolo*, 21:337–344, 1984.  
20  
21 [7] T.J.R. Hughes, L. Franca, and M. Balestra. A new finite element formulation for  
22 computational fluid dynamics: V. Circumventing the Babuška–Brezzi condition:  
23 A stable Petrov–Galerkin formulation of the Stokes problem accommodating  
24 equal–order interpolations. *Comput. Methods Appl. Mech. Engrg.*, 59:85–99,  
25 1986.  
26  
27 [8] L. Franca and T.J.R. Hughes. Two classes of mixed finite element methods.  
28 *Comput. Methods Appl. Mech. Engrg.*, 69:89–129, 1988.  
29  
30  
31  
32  
33  
34  
35  
36  
37  
38  
39  
40  
41  
42  
43  
44  
45  
46  
47  
48  
49  
50  
51  
52  
53  
54  
55  
56  
57  
58  
59  
60